THE ASTROPHYSICAL JOURNAL, 341:278–287, 1989 June 1

SPATIAL VARIATIONS OF THE 3 MICRON EMISSION FEATURES WITHIN UV-EXCITED NEBULAE: PHOTOCHEMICAL EVOLUTION OF INTERSTELLAR POLYCYCLIC AROMATIC HYDROCARBONS

T. R. GEBALLE,[1,2] A. G. G. M. TIELENS,[3,4] L. J. ALLAMANDOLA,[3] A. MOORHOUSE,[5] AND P. W. J. L. BRAND[5]

Received 1988 June 17; accepted 1988 October 28

ABSTRACT

We have obtained 3 μm spectra at several positions in the Orion Bar region and in the "Red Rectangle," the nebula surrounding HD 44179. The recently discovered weak emission features at 3.40, 3.46, 3.51, and 3.57 μm (2940, 2890, 2850, and 2800 cm^{-1}) are prominent in the Orion Bar region. The 3.40 μm and 3.51 μm features increase in intensity relative to the dominant 3.29 μm (3040 cm^{-1}) feature when going from the ionized to the neutral zone across the Orion Bar. The spectrum obtained in the Red Rectangle, 5″ north of HD 44179, is somewhat similar to those in the Orion Bar. However, only a weak and rather broad 3.40 μm feature is present at the position of HD 44179. These spectra demonstrate that some of the 3 μm emission components vary independently of each other and in a systematic way within UV-excited nebulae. This spatial variation is discussed in terms of the UV excitation and photochemical evolution of polycyclic aromatic hydrocarbons and related molecular structures. The spatial behavior of the weak emission features can be understood qualitatively in terms of hot bands of the CH stretch and overtones and combination bands of other fundamental vibrations in simple PAHs. An explanation in terms of emission by molecular sidegroups attached to the PAHs is less straightforward, particularly in the case of the Red Rectangle and other evolved, mass-losing objects. We estimate PAH sizes of 20–50 carbon atoms based on the susceptibility of PAHs to destruction by the far ultraviolet fields present in the Orion Bar and the Red Rectangle; the size range is similar to independent estimates made previously.

Subject headings: infrared: spectra — interstellar: molecules — nebulae: individual (Red Rectangle) — nebulae: Orion Nebula

I. INTRODUCTION

Recent observations of the 3 μm unidentified emission features found in many UV-excited nebulae have revealed that their spectra are considerably more complex than had earlier been appreciated. Although the dominant feature is the well-known 3.29 μm (3040 cm^{-1}) band, other features at 3.40, 3.46, 3.51, and 3.57 μm (2940, 2890, 2850, and 2800 cm^{-1}) are present in some objects and, in addition, the above features appear to be perched on a rounded "plateau" of emission, above the flat continuum, which extends approximately from 3.2 to 3.6 μm (3100 to 2800 cm^{-1}) (Geballe *et al.* 1985; de Muizon *et al.* 1986; Nagata *et al.* 1988). These features have been attributed to the vibrations of polycyclic aromatic hydrocarbons (PAHs) and to related species (e.g., Duley and Williams 1981; Leger and Puget 1984; Allamandola, Tielens, and Barker 1985; Sakata *et al.* 1984; de Muizon *et al.* 1986; Borghesi, Busoletti, and Colangeli 1987). However, precise molecular identifications of the emitting species are unknown.

Clues to the origin of the unidentified 3 μm emission features might be found, not only by accurate determination of their wavelengths and profiles or by studies of their intensity variations from source to source, as have been done previously (e.g., Geballe *et al.* 1985), but also by studying their spatial variations within extended sources. The most basic of the latter approaches is to study the dependence of feature strengths with distance from the star which pumps the emission. We have taken this last approach by obtaining spectra from 3.1 to 3.7 μm (3225 to 2700 cm^{-1}) at three locations in the Orion Bar which are located at different distances from the Trapezium stars, and by observing the Red Rectangle at two locations, one on HD 44179 itself and the other 5″ north of that star. At most of these locations fairly accurate UV fluxes can be estimated. Knowledge of the spectrum and flux of the ultraviolet radiation field is crucial to proper understanding of the physical conditions experienced by the emitting material and can be used to place constraints on the structure of the emitters. This information, in turn, sheds light on the spatial, chemical, and physical evolution of the band carriers and their environment.

II. OBSERVATIONS

All spectra were obtained at the United Kingdom 3.8 m infrared telescope on Mauna Kea, using the facility liquid and solid nitrogen–cooled grating spectrometer with a 5″ aperture. A spectrum of the Red Rectangle, which consists of 12 individual scans, was obtained in 1984 December, 5″ north of the central star HD 44179. A spectrum obtained with the aperture centered on the star already has been published (Geballe *et al.* 1985); however, a second such spectrum, obtained in 1987 January with the aperture centered on the star, is presented here. Total integration times were 18 and 1.1 minutes, respectively. During both of these measurements a chopper throw of ~40″ (EW) was used. Most of the Orion Bar measurements were obtained in 1986 December. The locations observed were position 4 (Aitken *et al.* 1979) and 10″ and 20″ south of this position. The number of independent spectra and the total integration times at these positions were 4, 6, and 7 and 15, 22, and 26 minutes, respectively. An additional 16 spectra at the 20″ south position were obtained in 1987 August and brought the total amount of observing time at this position to about

[1] Joint Astronomy Centre, Hilo, Hawaii.
[2] Foundation for Astronomical Research in the Netherlands (ASTRON).
[3] NASA/Ames Research Center.
[4] Space Sciences Laboratory, University of California (Berkeley).
[5] Royal Observatory Edinburgh.

TABLE 1

PEAK INTENSITIES OF EMISSION FEATURES

SOURCE	PEAK SPECTRAL INTENSITY OF FEATURE (10^{-17} W cm^{-2} μm^{-1})[a]				
	λ (μm) = 3.29	3.40	3.46	3.51	3.57
	ν (cm^{-1}) = 3040	2940	2890	2850	2800
Orion Position 4	3.9	0.50	0.20	0.17	0.10
Orion Position 4 (10″ S)	2.0	0.35	0.06	0.11	0.05
Orion Position 4 (20″ S)	0.50	0.13	<0.02	0.06	<0.02
Red Rectangle (HD 44179) ...	160.	10.	<5.	<5.	...
Red Rectangle (5″ N)	4.5	0.6	<0.2	0.2	<0.15

[a] Above continuum plus plateau for Orion Bar; above adjacent flux density levels for Red Rectangle.

2 hr. During all Orion Bar observations the chopper throw was 120″ (EW), so that the reference beam, although well within the ionized gas of the Orion Nebula, was off of the extended infrared continuum emission (see Sellgren 1981).

The spectra obtained 5″ north of HD 44179 in 1984 December were sampled every one-half resolution element. All other spectra were sampled every one-third resolution element. The spectral resolution was $\sim$0.0075 μm ($\sim$6.5 cm^{-1}); however, the spectra as shown here are Hanning-smoothed and have a resolution of $\sim$0.009 μm ($\sim$8 cm^{-1}).

The co-added spectra were divided by spectra of early-type stars observed during the same nights and were then multiplied by Planck functions corresponding to assumed fluxes and temperatures of these stars. For the Orion Bar measurements the calibration star was BS 1713 (L = 0.13, T = 10,000 K); for the Red Rectangle the stars were BS 2294 (L = 2.66, T = 18,000 K) and BS 1899 (L = 3.53, T = 25,000 K). The final spectra of the Orion Bar and of the Red Rectangle are displayed in Figures 1 and 2. The poor signal-to-noise ratios near 3.31 μm in these spectra are caused by strong absorption by telluric CH_4. Peak intensities of most of the emission features are given in Table 1.

III. DESCRIPTION OF SPECTRA

a) *Orion Bar*

The three spectra of the Orion Bar (Fig. 1) show the unidentified emission features superposed on weak continua. The spectrum at position 4 shows the well-known emission peaks at 3.29 and 3.40 μm and, in addition, peaks at 3.46, 3.51, and (marginally above the noise level) 3.57 μm. The latter three features were only recently discovered in IRAS 21282+5050 and in GL 437 by de Muizon *et al.* (1986) and have now also been identified in NGC 7027 (Nagata *et al.* 1988) as well as in the ρ Oph source, WL 16 (T. R. Geballe, unpublished). The "plateau" of emission extending from 3.2 to 3.6 μm is also evident in all three Orion Bar Spectra; such emission has also been observed previously in several sources (Geballe *et al.* 1985; de Muizon, d'Hendecourt, and Geballe 1987). The emission features in the Orion Bar decrease in intensity to the south of position 4. However, it is clear that the 3.40 and 3.51 μm features do not decrease as rapidly as the others. In particular the ratio of peak intensities of the 3.40 and 3.29 μm features is 0.13 at position 4, 0.18 10″ to the south, and 0.26 20″ to the south. The peak intensities of the 3.51 μm feature are 0.04, 0.06, and 0.12 relative to those of the 3.29 μm feature at these positions. Note that the ratios of the integrated intensity of each of the weaker features relative to the 3.29 μm feature is roughly a

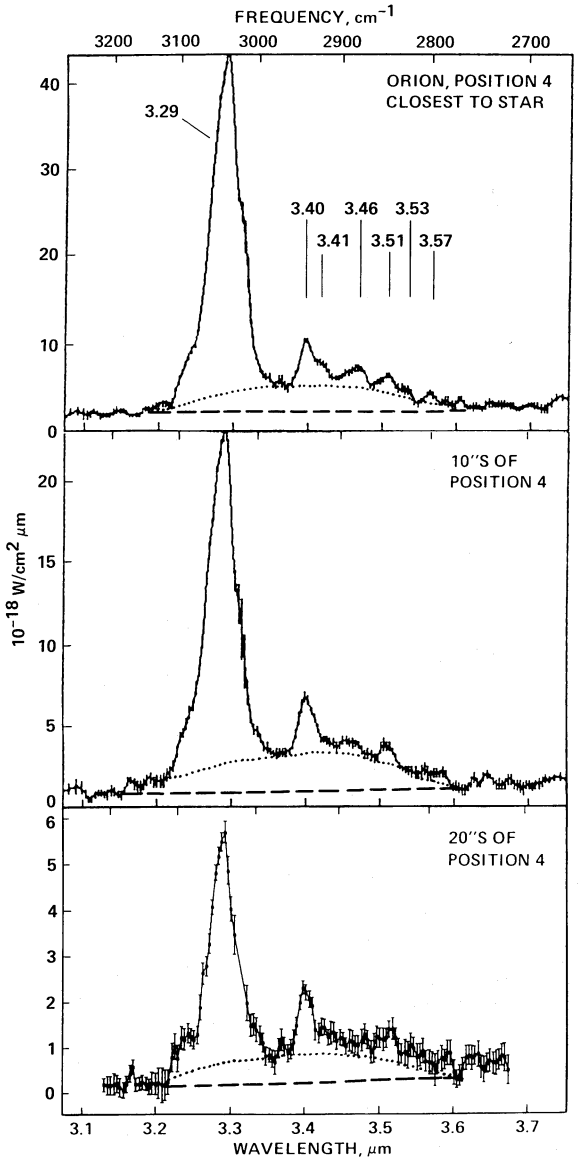

FIG. 1.—Spectra at 3 μm obtained in a 5″ beam at three locations within the Orion Bar. The spectral resolution is 0.009 μm. Dotted lines indicate the "plateau," dashed lines, the underlying continuum. Wavelengths of emission features are indicated in the top panel. Error bars are ± 1 σ.

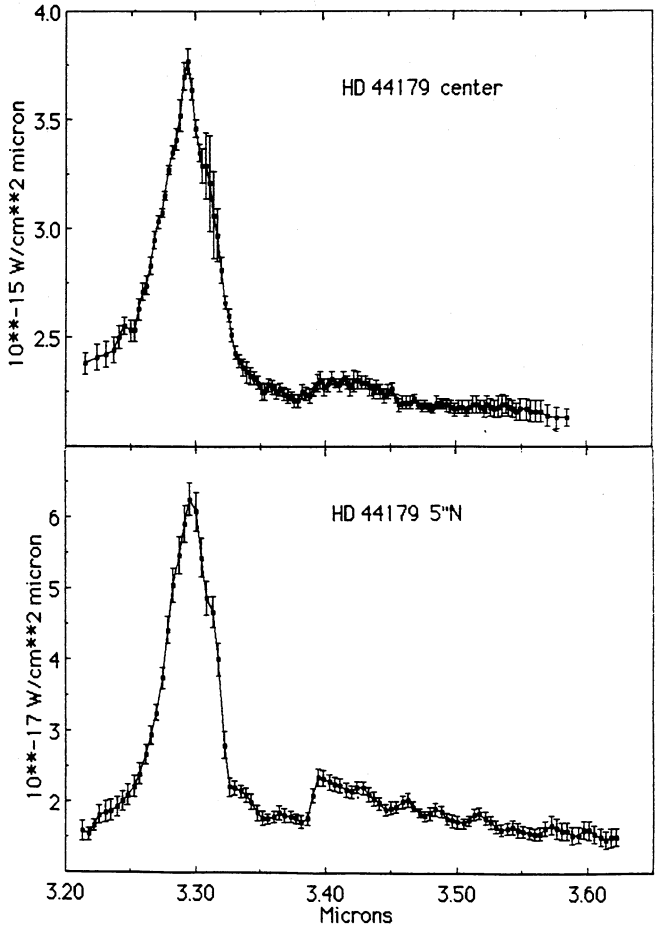

FIG. 2.—Spectra at 3 μm of the Red Rectangle obtained using a 5″ beam at the position of the exciting star and 5″ north of it.

factor of 2 less than the ratio of the peak intensities, because the width of the 3.29 μm emission is about twice that of each weaker feature.

In contrast to the behavior of the 3.40 and 3.51 μm features, the 3.46 μm component appears to be reduced in strength relative to the 3.29 μm feature 10″ south of position 4. At the 20″ south location there is no evidence for this feature at all. It also appears that the long-wavelength shoulders, present on the 3.40 and 3.51 μm features at position 4, decrease to the south. These shoulders may be due to independent and unresolved emission features at 3.415 and 3.53 μm.

b) Red Rectangle

Somewhat similar behavior to that in the Orion Bar is seen in the Red Rectangle spectra (Fig. 2). The spectrum observed at the position of HD 44179 shows a strong 3.29 μm feature and a weak, rather broad 3.40 μm feature superposed on a strong continuum. There is little evidence of the 3.2–3.6 μm plateau, although the 3.40 μm feature appears to be somewhat broader than in most other sources exhibiting it. At the off-star position the continuum, as judged by the flux densities at 3.2 and 3.6 μm, is reduced in spectral intensity by a factor of 150 (compared with a reduction of a factor of ~450 measured for unresolved sources), but the 3.29 μm feature has decreased by a factor of only 36. The ratio of peak intensity (above the continuum) of the 3.40 μm feature to that of the 3.29 μm features has markedly increased, from 0.06 at HD 44179 to 0.13 at the 5″ north position. The short-wavelength cut-on of the 3.40 μm feature appears to occur slightly shortward of the cut-on in Orion, and the peak of the feature shows a similar shift, although these differences are only marginally significant.

In addition to the 3.29 μm and 3.40 μm features, some weak spectral structures appear in the 5″ north spectrum. The weaker ones of these (3.43, 3.48, 3.57 μm) are probably the result of smoothing noise fluctuations in the spectrum. The most prominent of the weak features is at 3.51 μm; we believe that this feature is real. Note that this is one of the features seen to become relatively more prominent going across the Orion Bar, and that it is not seen at HD 44179. The reality of the next most prominent feature, at 3.46 μm, is questionable. Thus regarding the 3.29 μm, 3.40 μm, and 3.51 μm features, the trend is similar to that in the Orion Bar; the ratios of the latter two to the former increase with increasing distance from the stellar (UV) source. We also note that the 3 μm spectrum of HD 44179 obtained by Tokunaga *et al.* (1988) in a 2″.7 aperture is consistent with the above pattern; it shows no 3.40 or 3.51 μm features at all.

The present spectrum obtained at the location of HD 44179 (Fig. 2, *top panel*) shows some slight differences from a similar spectrum published by Geballe *et al.* (1985). Two faint emission features at 3.46 and 3.52 μm were marginally present (although not commented upon) in the earlier spectrum. Because of their proximity to two of the new features found by de Muizon *et al.* (1986), it was suggested by the latter authors that they might be the same ones. However, in the present spectrum of HD 44179 there is no evidence for these emission features. Moreover, it has been determined that spurious features at these wavelengths can be generated by dividing the spectrum of a bright continuum source by that of a late-type star which contains strong OH absorption lines (Tokunaga *et al.* 1988). The present spectrum of HD 44179 was divided by that of a hot star, and should contain no such spurious emission features.

c) Width of the 3.29 Micron Feature

Tokunaga *et al.* (1988) found that within their 2″.7 aperture the FWHM of the 3.29 μm feature in HD 44179 is only 0.023 μm (~20 cm^{-1}), roughly half that observed in other sources (Geballe 1984; Geballe *et al.* 1985; de Muizon *et al.* 1986; Nagata *et al.* 1988). Our spectra of the Orion Bar and of HD 44179 obtained in a 5″ beam, yield deconvolved FWHMS of ~0.040 μm (~37 cm^{-1}) and ~0.035 μm (~32 cm^{-1}), respectively. They were made at a lower spectral resolution than used by Tokunaga *et al.*, but one which easily resolved the feature. A recent (1988 October) spectrum of HD 44179, obtained by us in a 2″.5 aperture, confirms the narrow width found by Tokunaga *et al.*

There are some difficulties in determining the widths of 3.29 μm features, largely due to the deep and only partially resolved telluric CH_4 absorption on the long-wavelength side of the feature and the difficulty in determining the continuum level. These cause uncertainties of perhaps 0.005 μm (5 cm^{-1}) in the FWHMs. In determining the FWHMs given above, we have used a straight line to interpolate across the 3.31–3.32 μm interval. However, the Tokunaga *et al.* (1988) spectrum shows that the major difference between the profiles of the 3.29 μm feature in HD 44179 and in other objects occurs on the short-wavelength side of the 3.29 μm feature, where the atmospheric transmission is fairly good. The results of Tokunaga *et al.*, combined with ours, imply that the width of the 3.29 μm

feature can vary significantly, not only from source to source, but also with position in a source.

IV. DISCUSSION

The 3.29 μm feature has long been ascribed to emission from the C—H stretch in aromatic systems. Because of its high intensity relative to the lower frequency emission features, even far from the powering source, the carriers have to be small, containing 20–50 carbon atoms. Such molecular-sized aromatic entities are generically called polycyclic aromatic hydrocarbons (see Allamandola, Tielens, and Barker 1987 for a review).

Detailed spectra of the emission features in the 3 μm region should provide strong constraints on the carriers once laboratory spectra of realistic analogs become available. Within the framework of the PAH hypothesis, two general classes of interpretations for the weaker features (at 3.40, 3.46, 3.51, and 3.57 μm) already have been suggested. One is that some of these features are vibrational "hot bands" (e.g., $v = 2$–1 and 3–2) of the C—H stretch, blending with combination bands involving the low frequency C—C stretching and bending modes (Barker, Allamandola, and Tielens 1987). The other is that they are fundamental vibrations of molecular subgroups attached to the basic PAH structure (Duley and Williams 1981; de Muizon *et al.* 1986). Below we discuss the present spectra, which show positional variations in the relative strengths of these emission features, in the context of the above interpretations. At present each explanation can accommodate at least some of these observations, mainly because of the lack of laboratory data regarding these transitions in free PAHs. Of course, both explanations may actually contribute. Each explanation will be discussed in turn, within the context of what is currently known.

a) Vibrational Overtones and Hot Bands

In PAHs the fundamental C—H stretching vibration always occurs close to 3.29 μm. Anharmonicitiy of the vibrational potential as a function of atomic separation causes the transitions between higher adjacent vibrational levels (i.e., $v = 2$–1, $v = 3$–2, ...; often called "hot bands") to be shifted to successively longer wavelengths (lower frequencies). Two of the weak emission features observed in these and other objects, those at 3.40 and 3.51 μm, are quite close to, although not exactly at, the wavelengths of the 2–1 and 3–2 vibrational transitions of the C—H stretch in the small aromatic hydrocarbons, benzene, napthalene, and anthracene (Barker, Allamandola, and Tielens 1987). The anharmonicities of ionized and larger PAHs are not yet determined but are likely to be similar. It is possible that some of them might provide an exact match.

Absorption of an ultraviolet (UV) photon by a molecule is followed by a rapid redistribution of the photon energy among the various vibrational modes of the molecule. In the absence of any other deactivation route, this is followed by spontaneous deexcitation via infrared fluorescence. In the case of PAHs the latter process takes about 0.1 s. The PAHs which are believed to dominate the near-infrared and mid-infrared emission spectrum are thought to contain 20–50 carbon atoms (Leger and Puget 1984; Allamandola, Tielens, and Barker 1985). The larger molecules in this range contain many times more vibrational modes than can be simultaneously excited by a single UV ($h\nu < 13.6$ eV) photon. Thus population of high-energy modes such as C—H stretches in $v = 2$ or higher states will be unusual occurrences. However, because smaller PAHs have fewer modes, more frequent excitation above the $v = 1$ levels is expected for them. By the same token the smaller PAHs will also be more susceptible to photodissociation processes by the UV radiation field (Tielens *et al.* 1987).

For a highly vibrationally excited PAH, H loss is much more likely than fragmentation of its carbon skeleton. This is because the aromatic C—H bond strength ($\sim$4.5 eV) is significantly lower than the aromatic C—C bond strength (5.5 eV; cf. Table 2) and because at least two C—C bonds have to be broken simultaneously in order to lose a C atom. This requires 11 eV and a simultaneous bond excitation, a very improbable pair of events. Indeed, photodestruction is thought to play only a minor role in the breaking up of the carbon skeletons of interstellar PAHs (Crawford, Tielens, and Allamandola 1985). Emission of IR photons (IR fluorescence) and C—H bond rupture are competing relaxation mechanisms for highly vibrationally excited PAHs, but C—H bond rupture will dominate only when the amount of energy which is deposited in the molecule exceeds a critical threshold, E_c, whose value depends strongly on the size of the PAH and the internal excitation energy (Tielens *et al.* 1987). Small decreases in the size of the molecule or small increases in the internal excitation energy (e.g., the energy of the absorbed UV photon) will increase the probability of H loss by large factors. If reattachment of hydrogen is unlikely before the following UV photon with $E > E_c$ is absorbed, a small PAH eventually will be stripped of all of its H atoms.

Thus in regions with strong UV fields (e.g., at the surface of a molecular cloud or near the exciting star), interstellar PAHs with sizes below a critical value will be quickly dehydrogenated. Larger PAHs will not be dehydrogenated at all, but because these have many vibrational modes, little emission from the $v = 2$ or higher levels will occur, even in the intense UV field near the star. In a shielded environment, such as a molecular cloud (e.g., 20″ S of position 4 in the Orion Bar), or sufficiently far from the exciting star, rehydrogenation dominates over UV destruction, and all PAHs are completely hydrogenated. The smaller ones will be highly excited upon absorption of a UV photon and will emit strongly in the hot bands (i.e., near 3.40 and 3.51 μm). The resultant spectra of the region will be strongly dependent on the details of the PAH size distribution, but clearly, the observed spatial variations in the relative strengths of the 3.29, 3.40, and 3.51 μm bands shown in Figures 1 and 2 could be a natural consequence of this model.

To determine if this explanation is tenable, one must estimate how susceptible small PAHs are to dehydrogenation by UV radiation in the Orion Bar and the Red Rectangle. Within the framework of this model, the intensity ratios of the 3.29 to 3.40 μm features 10″ south of position 4 in the Orion Bar and 5″ north of HD 44179 in the Red Rectangle imply that the smallest hydrogenated PAHs contain about 15–20 carbon atoms, depending on the spectrum of absorbed UV photons (Barker, Allamandola, and Tielens 1987), In contrast, at position 4 and (especially) at HD 44179 the PAHs responsible for the 3.40 μm emission contain about 50% more C atoms. It is likely that this is because of the complete dehydrogenation of the smaller ones at the latter positions. Using quantum RRK theory (Barker 1983) one can calculate the C—H bond rupture rate as a function of PAH size and vibrational energy content. Tielens *et al.* (1987) show that the UV threshold for efficient dehydrogenation of PAHs containing about 18–20 carbon

TABLE 2

PHYSICAL PROPERTIES OF SIDEGROUPS ON POLYCYCLIC AROMATIC HYDROCARBONS

SIDEGROUP[a]	BENZENE DERIVATIVE	BOND[b]	ENERGY[b] (eV)	H STRETCHING MODE[c] (cm^{-1})	H STRETCHING MODE[c] (μm)	NOTES
Hydrogen	Benzene	C_6H_5-H	4.47	3030	3.29	
	Benzene	$C-C_5H_6$	11.0	...	...	1
Methyl	Toluene	$C_6H_5CH_2-H$	3.69	2925 s	3.42	2
	Toluene	$C_6H_5CH_2-H$		2870 m	3.48	
	Toluene	$C_6H_5-CH_3$	4.0	...	...	
Ethyl	Ethylbenzene	$C_6H_5CH_2-CH_3$	3.1	2926 s	3.42	
	Ethylbenzene	$C_6H_5CH_2-CH_3$	3.1	2853 m	3.51	
Methylene	Benzyl	$C_6H_5-CH_2$	4.9	2986	3.35	3, 4
	Benzyl	$C_6H_5-CH_2$	4.9	3062	3.27	
	Benzyl	C_6H_5CH-H	4.47	...	...	
Hydroxyl	Phenol	C_6H_5O-H	3.69	3610	2.77	5
	Phenol	C_6H_5-OH	4.5	...	...	
		C_6H_5-O	3.2	...	...	
Amine	Aniline	C_6H_5NH-H	3.47	3481	2.87	
	Aniline	C_6H_5NH-H	3.47	3395	2.95	
	Aniline	$C_6H_5-NH_2$	4.0	...	...	
Aldehydic hydrogen ..	Benzaldehyde	C_6H_5CO-H	3.21	2820	3.55	6
	Benzaldehyde	C_6H_5CO-H	3.21	2730	3.66	

[a] Structural formulae shown in Fig. 3.

[b] Energy of bond denoted by — (Benson 1965)

[c] Peak frequencies and wavelengths of H stretching modes (Bellamy 1966) Variation of about 10 cm^{-1} (0.01 μm) likely within a class of compounds. The indicators s and m denote strong and moderate intensities.

NOTES.—(1) Elimination of a carbon atom from the carbon backbone of a PAH requires two bonds to be broken simultaneously (thus 11.0 eV; Crawford *et al.* 1985). (2) Frequencies are for methyl groups directly attached to a benzene ring. In pure, saturated aliphatic hydrocarbons, the CH stretching frequencies are 2960 and 2870 cm^{-1} (3.38 and 3.48 μm). (3) Phenyl is a very stable radical (see text). (4) Theoretically calculated frequencies (Lutoshkin, Kotorlenko, and Krugylak 1972). Actual values may be slightly different. (5) Frequency and wavelength are for isolated hydroxyl group. If strong intramolecular hydrogen bonding occurs, peak shifts to $\sim$3200 cm^{-1} (3.13 μm). (6) Presence of two bands is due to a Fermi resonance of the aldehydic CH stretching mode with overtones of the bending vibrations.

atoms is about 75,000 cm^{-1} (1300 Å). Therefore to estimate the dehydrogenation rates in these objects one must know the UV flux in the 912–1300 Å range.

i) *The Orion Bar*

In the Orion Bar region most of the emission in the features originates in the neutral zone adjoining the H II region (Sellgren 1981; Bregman *et al.* 1988). The UV flux in the above band incident from θ^1 Ori C (T = 40,000 K) is estimated to be 3×10^{12} cm^{-2} s^{-1}, from the observed far-infrared intensity (cf. Werner *et al.* 1976; Tielens and Hollenbach 1985*b*). Multiplying this by an assumed PAH UV cross section (5×10^{-16} cm^2) yields an H loss rate of 1.5×10^{-3} s^{-1}. Assuming that rehydrogenation occurs with unit efficiency upon each H atom–PAH collision, the rehydrogenation rate is given by the expression, $R = 10^{-9} n$ s^{-1} (Tielens *et al.* 1987). At the Orion Bar, where $n = 10^5$, the rehydrogenation rate is then 10^{-4} s^{-1}. Clearly for such small PAHs, dehydrogenation dominates at position 4. For slightly larger PAHs ($\sim$25 C atoms), however, the critical UV photon energy for dehydrogenation falls above the Lyman limit, and they will be completely hydrogenated.

The emitting material 10″ and 20″ south of the bar is embedded in the neutral zone where the UV field is heavily attenuated. Assuming that the observed intensity of the 3.29 μm feature directly measures the flux of pumping UV photons, (i.e., that most of the 3.29 μm feature is due to large, completely hydrogenated PAHs), the UV field 20″ south of position 4 is eight times less than at position 4 (i.e., $\tau_{UV} \simeq 2$). The C—H rupture rate is then calculated to be about 2×10^{-4} s^{-1}, comparable to the rehydrogenation rate. If instead the 3.29 μm emission is dominated by smaller, partially dehydrogenated PAHs, then the UV field, and thus the C—H rupture rate, will be lower than estimated above. In either case it appears that dehydrogenation of PAHs close to the surface of a molecular cloud can quantitatively explain the observed spatial variations of the 3 μm spectra in the Orion Bar.

ii) *The Red Rectangle*

A similar analysis of the emission in the Red Rectangle leads to a slightly different model than above. Speckle observations at 2.2 μm have recently been made of this object, and show that its 1/*e* dimensions are 0.″8 × 0.″6 (Beckers *et al.* 1988). Our observations of the line-to-continuum ratio indicate that the 3.29 μm emission is slightly more extended. Therefore we evaluate the physical conditions at a distance of 1″ from HD 44179. For this star, we take the distance (330 pc) and luminosity (1×10^3 $L_\odot$) from Cohen *et al.* (1975), use T = 10,000 K to estimate that about 0.009 of the luminosity is radiated between 912 and 1300 Å (Kurucz, Peytremann, and Avrett 1974), and obtain a UV photon flux in this band of 6×10^{12} cm^{-2} s^{-1} at a radius of 1″. This flux is twice that at position 4 in Orion and implies that the H loss rate from PAHs containing 20 carbon atoms is $\sim 3 \times 10^{-3}$ s^{-1}. The hydrogen density

is not well known for this object. Hα measurements indicate a density of $\sim 100\ cm^{-3}$ at a distance of 15″ in the lobes (Warren-Smith, Scarrott, and Murdin 1981). Assuming that the nebula is due to a steady outflow from HD 44179, the density at 1″ is $2 \times 10^4\ cm^{-3}$, which translates into a rehydrogenation rate of $2 \times 10^{-5}\ s^{-1}$. Thus, in the region of brightest 3.29 μm emission, small PAHs probably are rapidly dehydrogenated; indeed, conditions appear to be considerably harsher than those in the Orion Bar.

It must be cautioned, however, that the geometry of the Red Rectangle suggests the presence of a bipolar flow; hence, the emission close to HD 44179 might actually originate within a circumstellar disk, whose density cannot easily be guessed. Whether the weakness of the 3.40 μm band close to HD 44179 can be attributed to photochemically driven dehydrogenation depends critically on the assumed density of the emitting circumstellar material.

A further problem is encountered in evaluating the conditions 5″ north of HD 44179. Due to geometric dilution, the UV field will have dropped by a factor of 25 compared to its value at $r = 1''$. In an outflow the density also will have decreased by this factor, so that the ratio of dehydrogenation and rehydrogenation rates should remain approximately constant within the nebula, until attenuation by dust becomes dominant. As the 3.29 μm feature has decreased by only a factor of 36 at the 5″ north position, significant attenuation of UV radiation by dust appears unlikely (i.e., $\tau_{UV} \sim 0.4$). Thus, unless the density is much higher 5″ north of HD 44179 than expected, the relative spatial variations of the 3 μm emission features in the Red Rectangle cannot be explained by the above simple model.

However, an important, and perhaps crucial, distinction between the conditions close to HD 44179 and those of the Orion Bar region is the intensity of the entire illuminating UV field (evaluated over all UV wavelengths longward of 912 Å). At a distance of 1″ from HD 44179 the absorption rate of all such UV photons by PAHs is about $0.1\ s^{-1}$, which is about 30 times larger than in the Orion Bar. Consequently, events governed by the absorption of two UV photons within a radiative relaxation time scale (i.e., $\Delta t_{abs} < t_{IR} = 0.1$ s) occur at least 10^3 times more frequently in the Red Rectangle than at position 4 in Orion. The increased likelihood of a high internal excitation energy, even larger than the Lyman limit, coupled with the (possible) low rehydrogenation rate, should result in the dehydrogenation of much larger PAHs close to HD 44179 than in the Orion Bar. Since the rate of two-photon events is proportional to r^{-4}, rehydrogenation will quickly dominate beyond a certain distance. Therefore two-photon events may be able to explain the weakness or absence of the 3.40 and 3.51 μm emission features close to HD 44179.

Thus within the framework of the "hot band" interpretation of the 3.40 and 3.51 μm features, the spatial dependence of these features both in Orion and in HD 44179 can be interpreted in terms of photochemically driven dehydrogenation of PAHs. The steep dependence of the dehydrogenation rate on the molecular size (Tielens *et al.* 1987) implies that the smallest PAHs, which are responsible for most of the emission in the 3.40 and 3.51 μm features, contain less than 25 C atoms. In the Red Rectangle, within 1″ of HD 44179, somewhat larger PAHs may also be dehydrogenated. The intensity ratio of the 3.29 μm and 3.40 μm features independently implies that the smallest hydrogenated PAHs present contain 15 to 20 carbon atoms (see, e.g., Barker, Allamandola, and Tielens 1987). The similarity of these size estimates is no coincidence, as both the emission in the hot bands as well as dehydrogenation depend on appreciable population of the higher vibrational levels of the CH stretching mode.

Finally, within this anharmonicity picture, not all of the weaker features in the 3 μm region are due to hot bands of the CH stretching vibrations. Some could be attributed to overtones (i.e., $v = 2$–0) and combination bands of the CC stretching vibrations, whose fundamentals occur in the 5–9 μm region. These would not be affected by dehydrogenation of the small PAHs. The weak 3.46 and 3.53 μm features in Orion may be examples of this emission since their spatial variations suggest a different origin than the 3.40 and 3.51 μm features. This idea is supported by laboratory spectra of several PAHs, some of which (i.e., coronene and pyrene) show weak, narrow absorption features at the former wavelengths as well as a broad, weak feature from 3.2 to 3.6 μm (Cyvin and Klaboe, reproduced in Allamandola, Tielens, and Barker 1987). The absence of these features in the spectrum of HD 44179 implies then that the PAH family responsible for the emission in this source is somewhat different from that in Orion. Such a compositional difference is also implied by the strikingly different 5–13 μm spectrum observed from this source (Cohen, Tielens, and Allamandola 1985; Cohen *et al.* 1986). Although the Orion Bar and the Red Rectangle are associated with objects in vastly different evolutionary stages, it is tempting to speculate that such compositional differences are created by the different intensities of the UV fields where most of the emitting PAHs are located.

b) Molecular Sidegroups

Figure 3 shows structural formulae of some typical sidegroups that can attach to PAHs. Table 2 lists physical properties of these sidegroups. Included in the table are the XH— stretching frequencies of each sidegroup when attached to benzene (i.e., each benzene derivative). In the sidegroup picture the best candidates for the bands in the 3.4–3.6 μm region are CH stretching vibrations of saturated aliphatic subgroups,

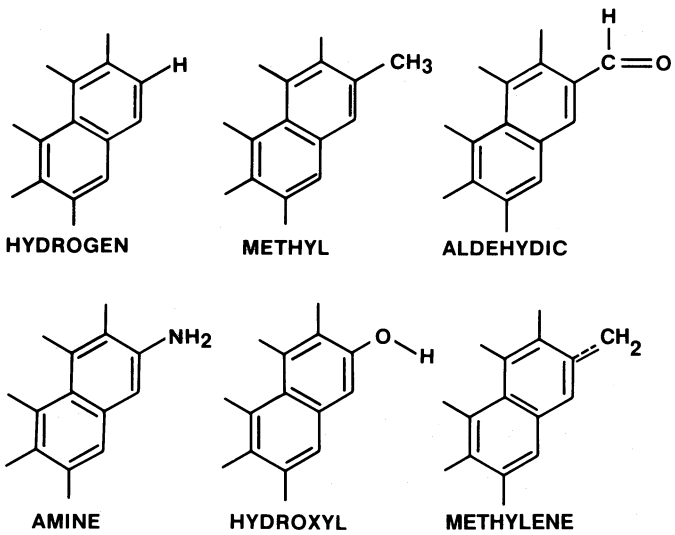

FIG. 3.—Structural formulae of some possible sidegroups on PAHs. The hexagonal networks schematically indicate the carbon backbone of the PAHs. Sidegroups, each of which would replace one H atom, are indicated only on one of the possible edge positions of a PAH. The "methylene" group actually refers to a relatively stable radical (see text).

such as $-CH_3$ and $-C_2H_5$ (Duley and Williams 1981; de Muizon *et al.* 1986; de Muizon, d'Hendecourt, and Geballe 1987). Although close, such saturated aliphatic hydrocarbon sidegroups do not provide an exact match to the observed spectral structure in the 3 μm region. However, it has been suggested that for ionized, dehydrogenated, or electronically excited PAHs these bands would be shifted and might provide a better match (de Muizon *et al.* 1986). Finally, one might perhaps expect the presence of sidegroups other than CH_2 and CH_3, notably CH and NH_2. However, due to their low binding energies, such sidegroups are very susceptible to photochemical destruction, and their expected intensities are small.

The present observations, particularly those of the Orion Bar, provide some constraints on sidegroup identifications. The observed 3.40 and 3.51 μm bands might be attributed to (shifted) methyl or methylene CH stretching vibrations. In contrast, since the observed 3.40 and 3.46 μm bands are decoupled, the latter cannot be the (shifted) methyl or methylene symmetric stretching vibration. Indeed, the difference in spatial behaviors of the 3.40 and 3.51 μm features relative to the other weak features (3.415 μm, 3.46 μm, 3.53 μm) is not readily explained within the sidegroup model (see below). However, even within the sidegroup model, $\Delta v = 1$ emission from higher vibrational levels of the CH stretching mode, and overtones and combination bands of the low-frequency CC stretching vibrations are expected at some level.

In the case that several of the weak bands are emitted by different molecular sidegroups, their intensities relative to other bands are a measure of the ratio of aromatic to aliphatic groups attached to the PAHs. The integrated band strengths for gas-phase PAHs with and without sidegroups are not known, but may be similar, as in the case of benzene derivatives (Gribov and Smirnov 1962; Wexler 1967). If so, the observed ratio (5–10) of the band intensity at 3.29 μm to the sum of those at longer wavelengths is simply the ratio of the number of aromatic to aliphatic H atoms in the emitting species. Assuming that each saturated aliphatic group contains three H atoms, the ratio of aromatic H atoms to aliphatic sidegroups is 15–30. This suggests that saturated aliphatic sidegroups are at best only a minor component of the IR-emitting PAHs. Attributing the emission to PAHs containing 20–50 carbon atoms with about 10–20 edge atoms results in an average of one sidegroup (other than H) per PAH, although one might construct models in which sidegroups dominate the peripheral groups on small PAHs and are absent on larger ones (see below).

In the sidegroup model, variations in the relative strengths of the features may be attributed to differences in the degrees to which different sidegroups survive exposure to the UV radiation field and the different rates of sidegroup reattachment after dissociation. It is therefore important to consider the binding energies of the various bonds involved with aliphatic sidegroups. These are summarized in Table 2. In view of the observed spectral structure, we restrict ourselves mainly to the aromatic hydrogen, methyl, and methylene groups. Examining Table 2, we infer that if there were just sufficient vibrational energy within the molecule to break a bond, the first ones to dissociate would be the C—H bond in the methyl side group and the C—C bond which connects methyl groups to a larger saturated aliphatic hydrocarbon sidegroup (i.e., $-CH_2-CH_3$). In both cases a very stable radical is produced because the unpaired electron on the remaining CH_2 sidegroup can participate in the aromatic π molecular orbital. In the case of methyl-benzene, the benzyl radical is formed. Due to the increased binding energy, further hydrogen loss from this stripped-down methyl group is about as likely as the loss of peripheral aromatic hydrocarbons. Thus, photochemistry will tend to convert saturated aliphatic hydrocarbon sidegroups into CH_2 radical sidegroups. Subsequently, the PAH may lose further hydrogens from this sidegroup, peripheral aromatic H atoms, or both, depending on the exact binding energies involved. Finally, loss of the carbon in the sidegroup may become important. As in the case of the anharmonic model, fragmentation of the carbon backbone of the PAH is expected to be of little importance.

i) *A Model for the Orion Bar Emission*

The above considerations suggest the following simple model for the photochemical evolution of PAHs in clouds near sources of intense far-UV radiation, such as in Orion. At a distance within the molecular cloud corresponding to $A_V \sim$ 5–10 mag, a small PAH (<25 carbon atoms) is likely to absorb a UV photon and lose an aromatic H during the lifetime of the region ($\sim 10^5$ yr for Orion). Because most of the hydrogen is locked up in H_2, abundances of atomic C and O are comparable to that of atomic H, while atomic N is somewhat less abundant (Tielens and Hollenbach 1985*a*). A PAH which has lost an H atom there is likely to grow an aliphatic sidegroup containing O, C, H, and, to a lesser extent, N. The expected sidegroups at this cloud depth may consist of an aliphatic carbon backbone with hydroxyl (e.g., OH), aldehydic (e.g., HC=O), amine (NH_2), and methyl and methylene (e.g., $-CH_3$, $-C_2H_5$) functional groups attached (cf. Fig. 3). Closer to the cloud surface ($A_V < 5$ mag) the UV field will photodissociate H_2 and atomic H will be more abundant than C and O, so the strengths of the sidegroup features relative to the 3.29 μm feature will decrease. In terms of the spatial behavior of the emission features, only the 3.40 and 3.51 μm features are even qualitatively consistent with the above model. However, since for small PAHs the photochemical rupture and rehydrogenation time scales are much shorter than the dynamical evolution of the Orion region, the composition of the sidegroups on PAHs should reflect the composition of the gas phase, and thus within the Orion Bar region observed ($A_V < 1$) only aromatic H groups are expected. One is then forced to assume that the smallest PAHs present in Orion have a time scale for photochemical evolution which is comparable to the lifetime of the region and, thus, will not have "equilibrated" with the gas phase. Possibly, the observed sidegroups might result from the photochemical evolution of PAHs accreted onto ice grain mantles (Allamandola 1988).

In principle, in the sidegroup model, the 3.4–3.6 μm features could originate in slightly larger PAHs than in the anharmonic model, as the average energy per oscillator is not required to be as high for emission in the CH_2 and CH_3 stretching vibrations as that needed to pump $v = 2$ and 3 levels of the aromatic CH stretch. Somewhat larger PAHs are also implicated if the observed variations are interpreted, as above, as implying a time scale of $\sim 10^5$ yr for photochemical evolution. Note that a short lifetime for the emitting PAHs immediately implies emission in CH stretch "hot bands," since a radiation field which destroys PAHs populates excited vibrational levels in the process. Thus, if $v = 1$–0 vibrations in sidegroups are the only cause of the weak 3 μm features, a long photochemical time scale for these PAHs is actually a necessity.

To summarize this discussion, in the Orion Bar the observed spatial intensity pattern of the 3.40 and 3.51 μm features relative to the 3.29 μm (fundamental CH stretch) feature is qualitatively similar to that expected from sidegroups, but the patterns seen for the other combinations of weak features do not match expected behavior. In addition, if the sidegroup model is valid, it appears that the PAHs must acquire sidegroups by some means other than UV photodehydrogenation followed by reactions with gas-phase species.

ii) *The Red Rectangle*

The situation in the Red Rectangle is quite different from that in Orion, because the 3 μm emitting material has been freshly synthesized from atomic gas formerly within HD 44179. In the harsh environment very close to the star, PAHs can only be formed without aliphatic sidegroups. As the PAHs move to greater distances from the star, conditions moderate to the point where sidegroups could survive. However, unless the carbon elemental abundance is extremely high (C/H $\gtrsim$ 1), complete hydrogenation is expected to dominate over sidegroup formation. Thus, we see no simple model that can account for the observed spatial variations in the 3 μm spectrum of the Red Rectangle within the context of the sidegroup model. In fact, this argument may apply to the structure in the 3 μm spectra in all outflow sources, such as planetary nebulae (NGC 7027) and other evolved objects (e.g., IRAS 21282+5050) which produce PAHs locally.

d) The ^{13}C—H *Stretch*

When the ^{12}C—H fundamental stretch occurs at 3.29 μm the ^{13}C—H fundamental stretch occurs at 3.42 μm. Thus ^{13}C may be responsible for the weak, long wavelength shoulder sometimes observed on the 3.40 μm feature. In Orion the emitting material is interstellar, where ^{12}C/^{13}C is $\sim$40 (e.g., see Hawkins and Jura 1987), in reasonable agreement with the strength of the 3.415 μm shoulder, after subtraction of the underlying broad component (plateau). In evolved objects mixing of CNO-processed material from the interior can lead to observed values of ^{12}C/^{13}C as low as $\sim$4. The spectrum of HD 44179 by Tokunaga *et al.* (1988), which shows no detectable 3.40 μm or 3.415 μm feature, demonstrates that ^{12}C/^{13}C is at least 50 in that object. CO observations of NGC 7027, another object which has a clear-cut 3.40 μm band, yield ^{12}C/^{13}C > 36 (Thronson 1983). Here, the ^{13}C may be responsible for the observed shoulder on the 3.40 μm emission feature.

e) Line Widths

In general the width of the 3.29 μm feature (FWHM $\sim$ 0.04 μm) is about twice that of the weaker features (FWHM $\sim$ 0.025 μm). The latter are somewhat difficult to determine accurately due to their blending with other weak features as well as their placement relative to the strong, underlying plateau, or "quasi continuum." We noted earlier that the 3.29 μm feature obtained with a 2".7 aperture centered on HD 44179 (Tokunaga *et al.* 1988) has a narrower width ($\sim$0.023 μm) than it does in our spectrum obtained with a 5" aperture, or in any other object observed to date. We also note that the 3.40 μm feature observed on HD 44179 (Fig. 2) is either a blend of more than one feature, or is unusually broad. Thus it appears that the widths of some of these features can vary substantially. In this section we will discuss possible interpretations of these observations, although we realize that further observational tests of these effects are warranted.

The width of an IR fluorescent feature is determined by the combined effects of the time-scale for intramolecular vibrational energy transfer (the Heisenberg uncertainty relation, $\Delta E\,\Delta t > \hbar$), intensity enhancement and blending with weaker modes that are close in frequency (i.e., Fermi resonance), and small shifts in frequency of the emitting mode between different molecules within the family of interstellar PAHs (Allamandola, Tielens, and Barker 1985). The first is generally cited for the widths of the narrower observed emission features (e.g., at 3.29 μm and 6.2 μm), while the last may be responsible for the broad 7.7 μm feature and the plateau of emission underneath the 11.3 μm feature (Allamandola, Tielens, and Barker 1985; Cohen, Tielens, and Allamandola 1985).

In the case that intramolecular energy transfer dominates, the width will reflect the density of states at the internal excitation energy and the coupling of these states with the emitting mode. Since the density of such states is a strong function of the excitation energy, one might expect that the widths of "hot bands" are much greater than those of the fundamentals. Likewise, given their similar excitation energies, one might expect that the CH stretching modes of CH_3 and CH_2 have widths similar to that of aromatic H. However, recent elegant studies of the line widths of overtones of the CH stretching modes in benzene (Reddy, Heller, and Berry 1982), as well as of other molecules, have shown that intramolecular energy transfer from a particular mode to the general thermal bath usually takes place through a very limited number of so-called doorway states. Apparently, partly due to near-energy resonance and partly due to the geometric structure of the molecule, the couplings to these states (other fundamental modes which are close in frequency, as well as overtones and combination bands of lower frequency fundamentals) are very strong, leading to a very fast energy transfer ($\Delta t \sim 10^{-13}$ s). The "doorway" states of the particular modes under consideration themselves couple rapidly with a slightly different set of "doorway" states, so that coupling of a particular vibrational mode with all of the other available modes in the thermal bath occurs on a much slower, diffusion time scale. Nevertheless, all modes communicate on a time scale much less than the typical time for IR emission (0.1 s), so that the assumption of statistical distribution of the available energy over all modes, used in calculating IR emission spectra (e.g., Allamandola, Tielens, and Barker 1985) is fully justified. The line width, however, is determined by those "doorway" modes that dominate the energy transfer from the energy level in question, and the observed widths of the 3.29 μm and 6.2 μm features is in general agreement with that expected from such time scales (Allamandola, Tielens, and Barker 1985).

Since the actual line width of a fluorescing mode depends to a large extent on the coupling to a few states, no large increase in line width with vibrational excitation energy is expected. In fact, experimental studies on benzene show that the width of CH stretching modes increases slightly for the first few modes, but decreases again for even higher modes. In view of the absence of laboratory data on astrophysically relevant PAHs, the decrease in line width for "hot bands" or sidegroups is not presently in conflict with the PAH hypothesis.

Although the line width of the 3.29 μm emission feature generally has been interpreted only in terms of energy transfer time scales, the observations of a large variation in the linewidth by Tokunaga *et al.* (1988) suggest that other contributions should be considered. In particular, close to HD 44179 perhaps even the largest PAHs contain only a few H atoms. Since the

3.29 μm line width is probably dominated by interactions with the stretching modes of other peripheral H atoms on the PAH, such an isolation in HD 44179 might lead to a narrower emission feature. Similarly, we note that in benzene a Fermi resonance between the CH stretching vibration and an overtone or combination band of CC stretching modes gives rise to a strong band at 3.25 μm (3080 cm^{-1}), close to that of the fundamental aromatic CH stretch (Herzberg 1945). The absorption spectrum of coronene and, to a lesser extent, pyrene, also show a strong overtone or combination band in this wavelength region (Cyvin and Klaboe, reproduced in Allamandola, Tielens, and Barker 1987). Blending of these two emission features and broadening by intramolecular energy transfer will give rise to an increased width and perhaps a slight shift in frequency of the CH stretching mode. The narrow 3.29 μm feature observed in a small beam around HD 44179 may then reflect a difference in composition of the PAH family responsible for the emission in this source. That is, the PAHs which dominate the emission within 1″ of HD 44179 may lack this overtone or combination band.

Such a compositional difference in the PAH family close to HD 44179 has already been suggested on the basis of its 5–8 μm spectrum, which shows a "7.7 μm emission feature" which peaks at much longer wavelengths (~8.0 μm) than in Orion (Cohen *et al.* 1986; Bregman *et al.* 1988; Allamandola, Tielens, and Barker 1987). This might mean that an overtone or combination band of the "7.7 μm" CC stretch is involved in broadening the 3.29 μm emission feature. In that case, one would expect that other sources that show a large wavelength shift in the peak of the 7.7 μm feature (e.g., CPD −56°8032 and He 2–113; Cohen *et al.* 1986) would also show a narrower 3.29 μm feature. The observed variations of this feature in the Red Rectangle would suggest that this Fermi responance is associated with the smallest PAHs. Very close to HD 44179, such species may have lost all of their aromatic H atoms, and, in the absence of the fundamental CH stretch, the intrinsic strengths of the overlapping overtone or combination band would decrease considerably. The 3.29 μm band would then be dominated by the CH stretch in somewhat large PAHs, which do not possess this Fermi resonance. Further laboratory and astronomical studies are needed to test these speculations.

V. CONCLUSION

The spectra presented here provide unambiguous evidence for the presence of several components to the 3 μm emission spectrum of UV-excited nebulae which vary independently of one another within each nebulae. The observed spatial behavior of these features, in conjunction with laboratory studies, suggests that the weak 3.46 and 3.53 μm features may be due to overtones and combination bands of low-frequency CC stretching vibrations. The observed spatial variations of the intensities of the 3.40 and 3.51 μm features relative to that of the 3.29 μm feature can be attributed to the photochemical evolution of the interstellar PAH family within UV-excited nebulae. In the Orion Bar, these two features can be either "hot bands" ($v = 2$–1, 3–2) of the CH stretch in simple PAHs (containing only aromatic H atoms), or emission in the CH stretching modes of saturated aliphatic subgroups. However, in the Red Rectangle, whose emitting material is mass recently lost from the central star, the same type of spatial variations appear difficult to explain in the context of the sidegroup model. Therefore, if the 3.40 and 3.51 μm features in the Orion Bar region are emitted by the same molecular species as they are in the Red Rectangle, one must seriously question whether sidegroups are involved. Given the paucity of relevant laboratory data and the ingenuity of theoreticians, however, both interpretations of these features still must be considered viable. The observed photochemical evolution of interstellar PAHs implies that the emission carriers are small (between 20 and 50 C atoms, depending on the model adopted). It is significant that estimates of PAH sizes obtained from this work are similar to those previously obtained from other considerations.

Progress in understanding the identifications and emission mechanisms of the various features awaits the availability of laboratory spectra. However, it is also important to quantitatively test further the dependency of the weak emission features on the UV radiation field. Additional observational tests might be carried out on planetary nebulae and other objects that show the 3 μm features. We note, for example that the 3 μm spectra of the planetary nebulae NGC 7027 and BD +30°3639 are considerably different (Geballe *et al.* 1985; Nagata *et al.* 1988). In BD +30°3639, where the 3.29 μm emission occurs rather close to the exciting star, the emission features in the 3.4–3.6 μm region are weak or absent, similar to HD 44179. In NGC 7027, where the emission occurs at an angular distance from the star perhaps 5 times greater (and hence where the UV radiation field is likely considerably less intense), the 3.4–3.6 μm features are relatively prominent. Spectra at different locations within the above objects might prove illuminating.

We wish to thank the staff of UKIRT for its support of this research. Some of the data described herein were obtained during UKIRT Service observing time. We are indebted to Professor Cyvin of Trondheim University, Norway for pointing out some important spectroscopic characteristics of condensed aromatics and to A. Tokunaga for a number of helpful comments. This work was partially supported by NASA grant 188-41-57 at NASA/Ames.

REFERENCES

Aitken, D. K., Roche, P. F., Spenser, P. M., and Jones, B. 1979, *Astr. Ap.*, **76**, 60.
Allamandola, L. J. 1988, in *Carbon in the Galaxy*, ed. J. Tarter (NASA CP), in press.
Allamandola, L. J., Tielens, A. G. G. M., and Barker, J. R. 1985, *Ap. J. (Letters)*, **290**, L25.
———. 1987, in *Polycyclic Aromatic Hydrocarbons and Astrophysics*, ed. A. Leger *et al.* (Dordrecht: Reidel), p. 255.
Barker, J. R., 1983, *J. Chem. Phys.*, **77**, 301.
Barker, J. R., Allamandola, L. J., and Tielens, A. G. G. M. 1987, *Ap. J. (Letters)*, **315**, L61.
Beckers, J. M., Christou, R. G., Probst, R. G., Ridgway, S. T., and von der Luhe, O. 1988, preprint.
Bellamy, L. J. 1966, *The Infrared Spectra of Complex Molecules* (New York: Wiley).
Benson, S. W. 1965, *J. Chem. Ed.*, **42**, 502.
Borghesi, A., Busoletti, E., and Colangeli, L. 1987, *Ap. J.*, **314**, 422.
Bregman, J., Allamandola, L. J., Tielens, A. G. G. M., Geballe, T. R., and Witteborn, F. C. 1988, *Ap. J.*, submitted.
Cohen, M., *et al.* 1975, *Ap. J.*, **196**, 179.
Cohen, M., Allamandola, L. J., Tielens, A. G. G. M., Bregman, J. D., Simpson, J., Witteborn, F. C., Wooden, D., and Rank, D. 1986, *Ap. J.*, **302**, 737.
Cohen, M., Tielens, A. G. G. M., and Allamandola, L. J. 1985, *Ap. J. (Letters)*, **199**, L93.
Crawford, M. K., Tielens, A. G. G. M., and Allamandola, L. J. 1985, *Ap. J. (Letters)*, **293**, L45.
de Muizon, M., d'Hendecourt, L. B., and Geballe, T. R. 1987, in *Polycyclic Aromatic Hydrocarbons and Astrophysics*, ed. A. Leger *et al.* (Dordrecht: Reidel), p. 287.

de Muizon, M., Geballe, T. R., d'Hendecourt, L. B., and Baas, F. 1986, *Ap. J. (Letters)*, **306**, L105.
Duley, W. W., and Williams, D. A. 1981, *M.N.R.A.S.*, **196**, 269.
Geballe, T. R. 1984, in *Workshop on Laboratory and Observational Infrared Spectra of Interstellar Dust*, ed. R. D. Wolstencroft and J. M. Greenberg (Edinburgh: Royal Observatory), p. 93.
Geballe, T. R., Lacy, J. H., Persson, S. E., McGregor, P. J., and Soifer, B. T. 1985, *Ap. J.*, **292**, 500.
Gribov, L. A., and Smirnov, V. N. 1962, *Soviet Phys.—Uspekhi*, **4**, 919.
Hawkins, I., and Jura, M. 1987, *Ap. J.*, **317**, 374.
Herzberg, G. 1945, *Molecular Spectra and Molecular Structure. II. Infrared and Raman Spectra of Polyatomic Molecules* (Princeton: van Nostrand Co.).
Kurucz, R. L., Peytremann, E., and Avrett, E. H. 1975, *Blanketed Model Atmospheres For Early Type Stars* (Washington: Smithsonian Astrophysical Observatory).
Leger, A., and Puget, J. L. 1984, *Astr. Ap.*, **137**, L5.
Lutoshkin, V. I., Kotorlenko, L. A., and Krugylak, Y. A. 1972, *Teor. Eksp. Khim.*, **8**, 542.
Nagata, T., Tokunaga, A., Sellgren, K., Smith, R. G., Onaka, T., Nakada, Y., and Sakata, A. 1988, *Ap. J.*, **326**, 157.
Reddy, K. V., Heller, D. F., and Berry, M. J. 1982, *J. Chem. Phys.*, **76**, 2814.
Sakata, A., Wada, S., Tanabe, T., and Onaka, T. 1984, *Ap. J. (Letters)*, **287**, L51.
Sellgren, K. 1981, *Ap. J.*, **245**, 138.
Thronson, H. A. 1983, *Ap. J.*, **264**, 599.
Tielens, A. G. G. M., Allamandola, L. J., Barker, J. R., and Cohen, M. 1987, in *Polycyclic Aromatic Hydrocarbons and Astrophysics*, ed. A. Leger *et al.* (Dordrecht: Reidel), p. 273.
Tielens, A. G. G. M., and Hollenbach, D. J. 1985*a*, *Ap. J.*, **291**, 722.
———. 1985*b*, *Ap. J.*, **291**, 747.
Tokunaga, A. T., Nagata, T., Sellgren, K., Smith, R. G., Onaka, T., Nakada, Y., Sakata, A., and Wada, S. 1988, *Ap. J.*, **328**, 709.
Warren-Smith, R. F., Scarrott, S. M., and Murdin, P. 1981, *Nature*, **292**, 317.
Werner, M. W., Gatley, I., Harper, D. A., Becklin, E. E., Loewenstein, R. F., Telesco, C. M., and Thronson, H. A. 1976, *Ap. J.*, **204**, 420.
Wexler, A. S. 1967, *Appl. Spectrosc. Rev.*, **1**, 9.

L. J. ALLAMANDOLA and A. G. G. M. TIELENS: NASA/Ames Research Center, MS 245–6, Moffett Field, CA 94035

P. W. J. L. BRAND and A. MOORHOUSE: Royal Observatory, Blackford Hill, Edinburgh EH9 3HJ, Scotland

T. R. GEBALLE: Joint Astronomy Centre, 665 Komohana Street, Hilo, HI 96720